Proceedings of CLIMA 2013, the 11th REHVA World Congress and the 8th Conference on Indoor Air Quality, Ventilation and Energy Conservation in Buildings, June 16-19, Prague, Czech

Validation of a Fast Fluid Dynamics Program for Simulating Natural Ventilation in Buildings

Mingang Jin[#1], Qingyan Chen[#1] and Wangda Zuo*[2]

[#]*School of Mechanical Engineering, Purdue University, West Lafayette, IN 47907, USA*

[1] jin56@purdue.edu

[2] yanchen@purdue.edu

**Environmental Energy Technologies Division, Lawrence Berkeley National Laboratory, Berkeley, CA 94720, USA*

[3]wzuo@lbl.gov

Abstract

Natural ventilation is a sustainable building technology that can provide good indoor environment and save energy. The application of natural ventilation in buildings requires a careful design in the early design phase, and simple, fast design tools are highly needed. As an intermediate approach between computational fluid dynamics (CFD) and multi-zone model, fast fluid dynamics (FFD) can provide informative airflow information with a speed of 15 times faster than the laminar CFD so that it could be a potential design tool for natural ventilation. This study thus evaluated the performance of FFD for simulating natural ventilation. The FFD was validated with three cases representing natural ventilation with different driven forces: (1) wind-driven natural ventilation through a scaled building model; (2) wind-driven natural ventilation under different wind direction through a full scale building with partitions; (3) buoyancy-driven single-sided natural ventilation in an environmental chamber with a large opening. From comparing the results predicted by FFD and the experimental data, this study found that the FFD was capable of predicting main air flow feature and ventilation rate with reasonable accuracy for the wind-driven or buoyancy-driven natural ventilation in buildings.

Keywords: Fast fluid dynamics; Natural ventilation

1. Introduction

Natural ventilation is a sustainable building technology that can provide a good indoor environment and save energy. However, the design of natural ventilation is more difficult than that for mechanical ventilation because the driving force of natural ventilation is complicated [1] and its performance is highly dependent on various factors, such as outdoor microclimate, building shape and orientation. A design tool that can predict the influence of these factors on natural ventilation will be necessary for architects to optimize the natural ventilation design.

Many methods have been developed to predict natural ventilation, such as analytical and empirical models for single-sided or cross natural ventilation with simple geometry. With simple equations, the analytical and empirical expressions developed in the literature are easy to apply and quick to compute, but they are only suitable for simple or single-zone buildings. For buildings with multiple rooms, multi-zone models have been proposed to predict the natural ventilation rate through the buildings. But the multi-zone model may not be accurate for predicting airflows with a strong temperature gradient or with a strong momentum effect in a zone. Also, this model cannot provide air velocity or resolve airflow patterns or temperature distributions within a zone, which are very important for analyzing the indoor air quality and thermal comfort. On the other hand, with applying appropriate turbulence models, computational fluid dynamics (CFD) can accurately provide the distributed air velocity and temperature within zones. It has been successfully used for analyzing the performance of natural ventilation. However, due to its large demand for computation, running the CFD analysis is time consuming and is mainly used for final design evaluation and research projects. For early stages of building design, it would be impractical for architects to evaluate the performance of each natural ventilation design by using CFD. Thus, an ideal approach for early design should be able to provide rich airflow information in and around buildings as the CFD does, and should be as efficient as the multi-zone model.

As an intermediate approach between the multi-zone model and CFD, fast fluid dynamics (FFD) can provide fast simulation of airflow in buildings [2,3]. Thus, it has the potential for natural ventilation design. Previous study [4] showed that FFD could provide reliable simulations for indoor airflows at a speed about 15 times faster than CFD. However, FFD has not been applied to simulating natural ventilation, so it is necessary to evaluate its performance for the current application. This forms the basis of the current investigation as reported in this paper.

2. Research Method

2.1 Fast Fluid Dynamics

Fast fluid dynamics was originally developed by Stam [5] for computer graphics, simulating efficiently incompressible fluid flows. To achieve high computational efficiency, FFD applies a three-step time-advancement scheme to solve the Navier-Stokes and continuity equations for incompressible viscous fluid:

$$\frac{\partial U_i}{\partial t} + U_j \frac{\partial U_i}{\partial x_j} = -\frac{1}{\rho}\frac{\partial p}{\partial x_i} + \upsilon \frac{\partial^2 U_i}{\partial x_j \partial x_j} + \frac{1}{\rho} F_i, \qquad (1)$$

$$\frac{\partial U_i}{\partial x_i} = 0, \tag{2}$$

where i, j = 1, 2, 3. U_i is the i^{th} component of the velocity vector, p pressure, ρ density, F_i i^{th} component of body forces, and xi ith component of spatial coordinates, respectively. The three-step time-advancement scheme splits the Navier-Stokes equations into three discretized equations:

$$\frac{U_i^* - U_i^n}{\Delta t} = -U_j^n \frac{\partial U_i^n}{\partial x_j}, \tag{3}$$

$$\frac{U_i^{**} - U_i^*}{\Delta t} = \upsilon \frac{\partial^2 U_i^{**}}{\partial x_j \partial x_j} + \frac{1}{\rho} F_i, \tag{4}$$

$$\frac{U_i^{n+1} - U_i^{**}}{\Delta t} = -\frac{1}{\rho} \frac{\partial p}{\partial x_i}, \tag{5}$$

where U^n and U^{n+1} represent the velocity at the previous and current time step, respectively, and U* and U** are the intermediate velocity obtained from solving (3) and (4), respectively. FFD first solves (3) explicitly for advection by using a first-order semi-Lagrangian method. By applying the Lagrangian advection on the Eulerian grid, the semi-Lagrangian method can achieve enhanced stability at larger time steps. To solve U* in equation (3), FFD uses backward trajectory to determine the departure locations of particles arriving at the grid cells at the end of each time step. The velocity at the grid cells can then be updated with the velocity at the departure point, which can be interpolated from the velocity at surrounding grid cells. U* can be expressed by the following equation:

$$U_i^*(x_j) = U_i^n(x_j - \Delta t U_j^n), \tag{6}$$

where $U_i^*(x_j)$ is U_i^* at location $x_j = (x_1, x_2, x_3)$. Thereafter, FFD solves the diffusion equation with a source term by a fully implicit scheme to obtain another intermediate velocity, U**. Finally the pressure projection is conducted to project the intermediate velocity field into a space of divergence free vector field to obtain pressure and updated velocity. By substituting equation (5) into equation (2), the following Poisson equation can be derived:

$$\frac{\partial^2 p}{\partial x_j \partial x_j} = \frac{\rho}{\Delta t} \frac{\partial U_i^{**}}{\partial x_i}. \tag{7}$$

By solving equation (7) for pressure, FFD updates the velocity field with equation (5) to obtain U^{n+1}. After obtaining the velocity field, transport equations for other scalars can be further solved in a similar manner:

$$\frac{\partial \Phi}{\partial t} + U_j \frac{\partial \Phi}{\partial x_j} = \Gamma \frac{\partial^2 \Phi}{\partial x_j \partial x_j} + S, \tag{8}$$

where Φ is the scalar to be solved, Γ the transport coefficient, and S the source term, respectively.

Although FFD solves the Navier-Stokes equation as CFD does, the computing speed is more important for FFD than for CFD. The semi-Lagrangian method that is applied for solving the advection equation allows FFD to adopt larger time steps, so the simulation by FFD can advance much faster than that by CFD. FFD also uses simple and lower order schemes to improve computational efficiency. For example, it uses linear interpolation instead of higher-order interpolation in the semi-Lagrangian method. The pressure projection also uses only the first-order projection. FFD further increases its computing speed by reducing the iterations for solving the coupled momentum and continuity equations. In FFD, to obtain a more converged solution for satisfying both momentum and continuity equations inner iterations are not applied for each time step as in CFD. As a result, FFD has a lower computing cost but less accuracy than CFD.

Because accuracy is not the objective of FFD, FFD maintains its simplicity without integrating any turbulence models in the current study. Instead, a previous study shows that the lower order scheme applied in FFD can generate high numerical viscosity, which can be used as a substitute for turbulent viscosity. Numerical viscosity is dependent on grid size and will decrease when the grid is refined.

2.2 Boundary Conditions

In FFD, paired boundary conditions for both velocity and pressure are required to solve implicit diffusion equations and the Poisson equation. This study applied three typical flow boundary types: inlet, outlet, and solid wall. At the inlet boundary, a Dirichlet boundary condition was applied for velocity. In addition, FFD used the physical velocity boundary condition as a boundary condition for intermediate velocity as follows:

$$U_i^{**} = U_i^{n+1} = U_{inlet}, \tag{9}$$

where Uinlet is the given velocity at the inlet. The Neumann boundary condition for pressure was derived from equations (5) and (7):

$$\frac{\partial p}{\partial n}\Big|_b = 0, \tag{10}$$

where n is the local normal to the studied surface. At the outlet, FFD applied local mass conservation for the outflow boundary for velocity. Similarly, Neumann boundary conditions can be derived for pressure at outflow boundaries as shown by equation (10).

This investigation applied no-slip wall boundary conditions for the solid wall. The air velocity at a solid wall boundary is zero, as shown by equation (11):

$$U_i^{**} = U_i^{n+1} = U_{wall} = 0, \tag{11}$$

where U_{wall} is the air velocity at the wall. Also, equation (10) was applied as boundary condition for the pressure.

3. Results and Discussion

This study evaluated the performance of FFD for simulating natural ventilation with different driven forces. First, this investigation applied FFD to wind-driven, single-sided, and cross natural ventilation in a wind tunnel. And then FFD was then used to simulate wind-driven, natural ventilation through a four-zone, full-scale building in a wind tunnel, which is a more complicated case. The ventilation rate under different wind directions was computed by FFD and compared with the experimental data. This study further applied FFD to simulate buoyancy-driven, single-sided ventilation in a full-scale chamber.

3.1 Wind-driven, Natural Ventilation in a Wind Tunnel

The first case study is a wind-driven, natural ventilation case based on the experiment conducted by Jiang et al.[7]. The experiment employed a scaled building model with openings and a wind tunnel. Three different types of wind-driven, natural ventilation were studied: single-sided ventilation with a windward opening, single-sided ventilation with leeward opening, and cross ventilation with openings in both windward and leeward walls. The building model is depicted in Fig. 1(a). The experiment measured the mean velocity distribution along ten vertical lines in the streamwise direction, and their locations are shown in Fig. 1(b).

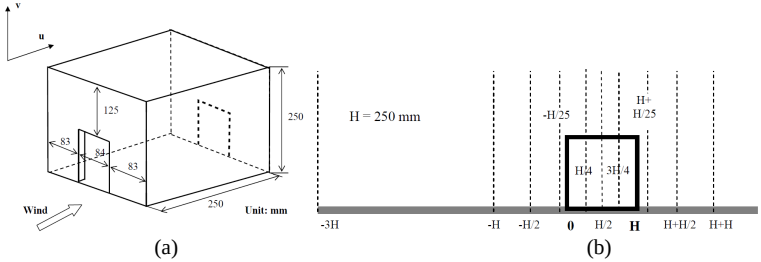

Fig. 1 Schematic view of the (a) building model and (b) measurement positions (Jiang et al.[7])

This study compared the velocity profiles along the streamwise locations, as shown in Fig. 2. The results computed by FFD were also compared with the CFD results by Alloca [8] for the three cases. At the upstream of the building (X = -H/25), the velocity profiles predicted by CFD agreed very well with the experimental data in all three cases. FFD also computed velocity profiles close to the experimental data with some discrepancies at Z=0.25. For the velocity distribution in the building model (X = H/2), both FFD and CFD predicted low velocity in the building for single-sided ventilation. For cross ventilation, FFD could predict the velocity variation in the building, but the agreement was poorer than CFD. Also, at the top of the building, FFD was not able to capture the recirculation

(negative velocity around Z=0.25) as CFD did. At the region near the leeward wall (X = H+H/25), the results simulated by CFD and FFD agreed well with the experimental data. However, at the downstream of the building model (X = H+H/2), neither CFD nor FFD could not obtain accurate simulation results for the three cases. Alloca [8] also made a similar conclusion, that CFD with the RANS turbulence model could not predict the velocity distribution well for the wake region behind the building model. Jiang et al. [7] found that only LES can achieve an accurate prediction. Through the comparison above, this study found that FFD could predict the main airflow distribution for wind-driven, single-sided, and cross natural ventilation with a lower accuracy than CFD with turbulence models.

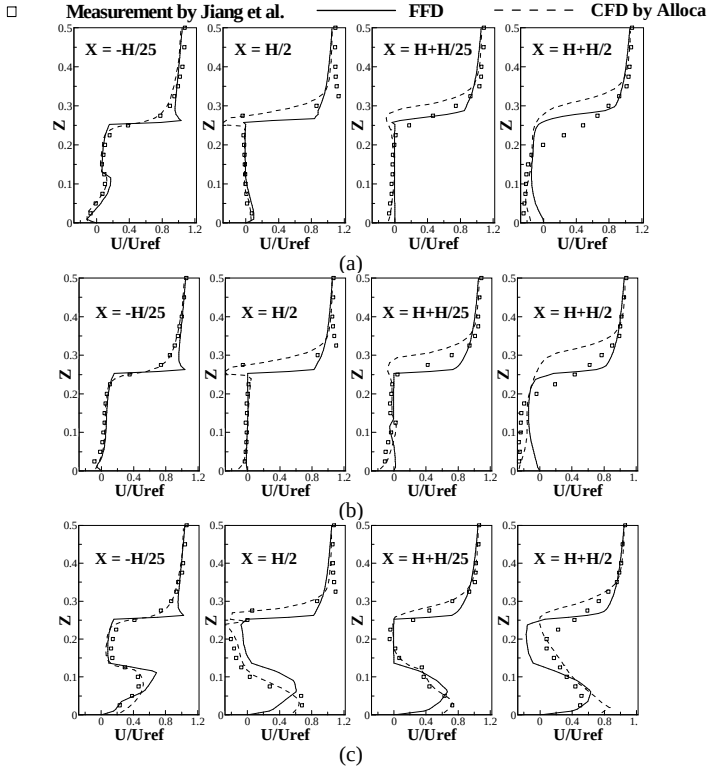

Fig. 2 Mean velocity distributions in the streamwise direction for (a) single-sided, windward ventilation, (b) single-sided, leeward ventilation, and (c) cross ventilation

3.2 Cross Ventilation Through a Four-zone Building Model

This study further tested FFD for prediction of the impact of wind direction on wind driven natural ventilation. Sawachi et al. [9] measured

discharge coefficients at the building openings under different wind directions using a full-scale building model with four sub zones in a large wind tunnel, as shown in Fig. 3. The building model can be rotated in the wind tunnel to study the impact of different wind directions on cross ventilation. This study applied FFD to simulate the airflow path through the building model and the ventilation rate under cross ventilation with different wind directions.

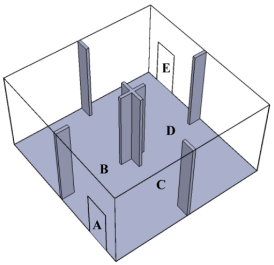

Fig. 3 Sketch of the four-zone building model

The wind direction would change the pressure difference of the two openings and thus influence the ventilation rate through the building. Design tools should be able to predict the impact of wind direction on ventilation rate. Fig. 4 compares the ventilation rate computed by FFD with the corresponding measured data. The ventilation rate was highest when the wind direction was normal to the opening A, and lowest when the wind direction was parallel to opening A. FFD could predict this trend and the calculated ventilation rate showed reasonable agreement with the experimental result. Thus, FFD was capable of predicting the impact of wind direction on natural ventilation.

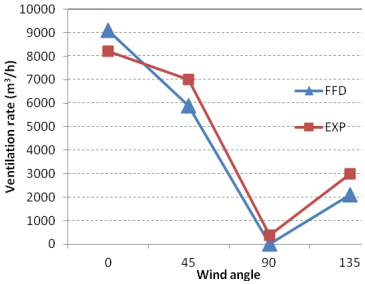

Fig. 4 Comparison of ventilation rates with different wind angles by FFD and the data from Sawachi et al.[9]

3.3 Buoyancy-driven, Single-sided Natural Ventilation

To validate the performance of FFD for buoyancy-driven, natural ventilation, this investigation used the experimental case by Jiang et al.[10]. The experiment used a test chamber in a laboratory to simulate the indoor environment and the laboratory space to simulate the outdoor environment. A 1500 W baseboard heater was placed in the test chamber to generate buoyancy force. The door was open to simulate buoyancy-driven, single-sided ventilation. Fig. 5(a) shows the layout of the chamber and the laboratory and their dimensions. In the experiment, the air velocity and temperature distributions were measured at five different locations as shown in Fig. 5(b).

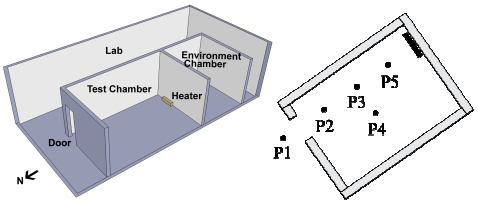

(a) (b)

Fig. 5 Sketch of (a) the layout of the laboratory and (b) measurement positions

Fig. 6 compares the airflow field simulated by FFD and CFD. The flow pattern predicted by FFD was in good agreement with that predicted by CFD. Both FFD and CFD predicted the high speed regions along the top and bottom parts of the room, and the plume above the heat source. Although the simulated flow pattern outside the door was slightly different between FFD and CFD, FFD captured the main airflow features of single-sided natural ventilation just as CFD did.

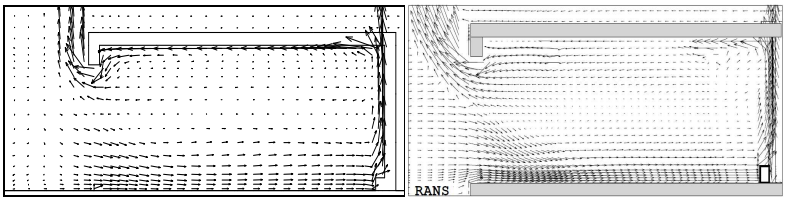

(a) (b)

Fig. 6 Comparison of airflow patterns simulated by (a) FFD and (b) CFD by Jiang [11]

Fig. 7 compares the velocity profiles computed by FFD and CFD with the corresponding experimental data. In the chamber, the velocity profiles computed by FFD and CFD showed acceptable agreement with the data. Both FFD and CFD predicted high velocity near the ceiling and the floor and

low velocity at the middle height inside the chamber. For the airflow outside the door (Position P1), neither FFD nor CFD could predict the velocity variation over the door with high accuracy. FFD and CFD showed similar accuracy for predicting airflow distribution for the buoyancy-driven natural ventilation.

Table 1 compares the air change rates computed by FFD and CFD with the experimental data. Both FFD and CFD provided reasonable estimates for air change rates induced by buoyancy-driven natural ventilation, and FFD performed rather well in this case.

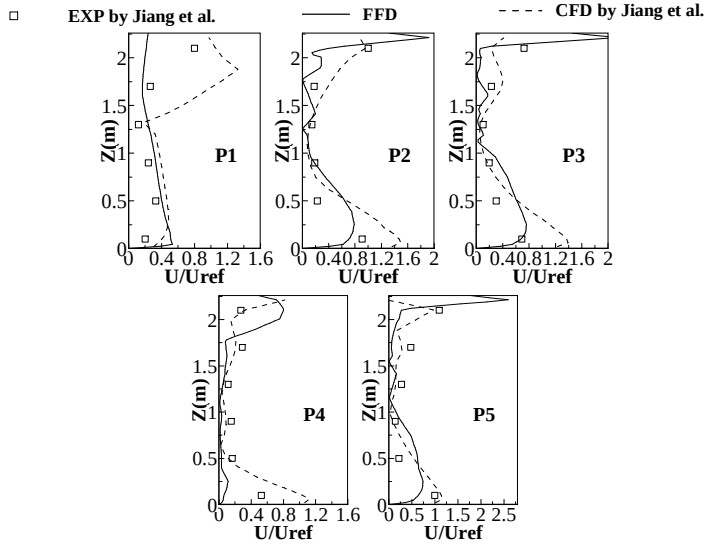

Fig. 7 Comparison of the computed velocity profiles with the experimental data at the five measurement positions

Table 1 Air change rates for single-side natural ventilation

	Experimental measurements	CFD	FFD
Air change rate (ACH)	9.18-12.6	15.2	9.36

For the temperature distribution in the chamber, Fig. 8 compares the computed temperature profiles by FFD and CFD with the experimental data at the five measurement positions. The thermal stratification was clearly predicted by both FFD and CFD. Although FFD predicted a higher temperature at the ceiling level, the temperature distribution simulated by FFD was in reasonable agreement with the experimental data. Also, the

largest thermal stratification computed by FFD occurred in the middle section of the room, which was consistent with the experimental data and the CFD simulation by Jiang.

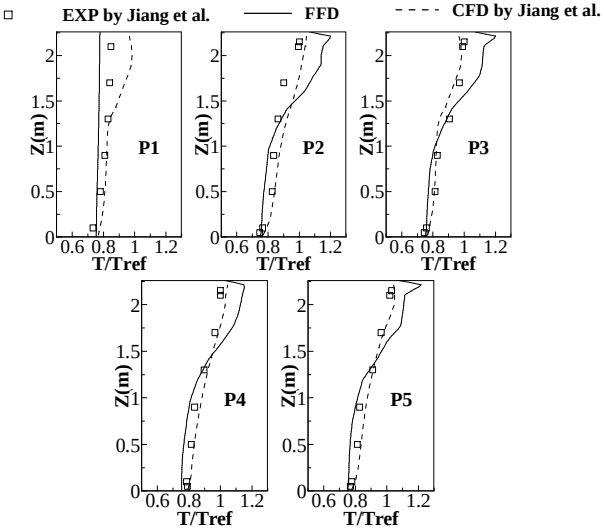

Fig. 8 Comparison of the computed velocity profiles with the experimental data at the five measurement positions

4. Conclusions

This study validated FFD performance for simulating different types of natural ventilation. Through the test, this study led to the following major findings:

For wind-driven, single-sided natural ventilation and cross natural ventilation, FFD can accurately predict the velocity distribution on the upstream side of a building. However, FFD was not as accurate as CFD with a RANS model for simulating airflow distribution inside and on the downstream side of the building. Nevertheless, FFD can still capture the main airflow feature. FFD can determine the impact of wind direction on cross natural ventilation. The ventilation rate computed under different wind directions agreed reasonably well with the corresponding experimental data.

For buoyancy-driven, single-sided natural ventilation, FFD can predict the airflow pattern in the room generated by a heat source as well as thermal stratification in the room. The air change rate calculated by FFD also agreed well with the experimental data.

Acknowledgement

This work was supported by the U.S. Department of Energy through the Energy-Efficiency Building Hub program led by Pennsylvania State University.

References

[1] Linden PF. The fluid mechanics of natural ventilation. Annual Review of Fluid Mechanics 1999; 31(1):201–238.
[2] Zuo W, Chen Q. Fast and informative flow simulations in a building by using fast fluid dynamics model on graphics processing unit. Building and Environment 2010; 45(3):747–757.
[3] Zuo W, Chen Q. Real-time or faster-than-real-time simulation of airflow in buildings. Indoor Air 2009; 19(1):33–44.
[4] Jin M, Zuo W, Chen Q. Validation of three dimensional fast fluid dynamics for indoor airflow simulations. In: Proceedings of 2nd international conference on energy and environment. Boulder,Colorado. 2012.
[5] Stam J. Stable fluids. In: The 26th annual conference on computer graphics and interactive techiniques. Los Angeles: ACM Press, 1999. p. 121–128.
[6] Staniforth A, Côté J. Semi-Lagrangian integration schemes for atmospheric models—a review. Monthly Weather Review 1991; 119(9):2206–2223.
[7] Jiang Y, Alexander D, Jenkins H, Arthur R, Chen Q. Natural ventilation in buildings: measurement in a wind tunnel and numerical simulation with large-eddy simulation. Journal of Wind Engineering and Industrial Aerodynamics 2003; 91(3):331–353.
[8] Allocca C. Single-sided natural ventilation: design analysis and general guidelines. Massachusetts Institute of Technology, 2001.
[9] Sawachi T, Narita K, Kiyota N, Seto H, Nishizawa S, Ishikawa Y. Wind pressure and airflow in a full-scale building model under cross ventilation. The International Journal of Ventilation 2004; 2(4):343–358.
[10] Jiang Y, Chen Q. Buoyancy-driven single-sided natural ventilation in buildings with large openings. International Journal of heat and mass transfer. 2003;46(6):973–988.
[11]Jiang Y. Study of natural ventilation in buildings with large eddy simulation. Massachusetts Institute of Technology, 2002.